TABLE 2
Sensitivity, specificity, PPV, and NPV of CRP and T-bil for several threshold values

Cutoff value	Sensitivity (95% CI)	Specificity (95% CI)	PPV (95% CI)	NPV (95% CI)
CRP (mg/L)				
6.0	100 (95.8–100.00%)	55.3 (44.1–66.1%)	69.4 (60.4–77.3%)	100 (92.4–100.00%)
10	97.7 (91.8–99.7%)	76.5 (66.0–85.0%)	80.8 (71.9–87.8%)	97 (89.6–99.6%)
24	91.9 (83.9–96.7%)	90.6 (82.3–95.8%)	90.8 (82.7–95.9%)	91.7 (83.6–96.6%)
T-bil (mg/dL)				
0.6	96.2 (86.0–97.9%)	50 (38.8–61.3%)	64.7 (55.2–73.3%)	89.1 (76.4–96.3%)
0.9	73.8 (62.7–83.0%)	95.1 (88.0–98.6%)	93.7 (84.5–98.2%)	78.8 (69.4–86.4%)
1.1	65 (53.5–75.3%)	97.6 (91.5–99.6%)	96.3 (87.2–99.4%)	74.1 (64.8–82.0%)

95% CIs were calculated using MedCalc (http://www.medcalc.org/calc/diagnostic_test.php).

Japanese patients with malaria who are non-immune to malaria (non-immune malaria patients) were compared with patients from endemic areas that are assumed to be semi-immune to malaria (semi-immune malaria patients) (Figure 2). The CRP values of semi-immune malaria patients were significantly higher than the values of non-immune patients (median [IQR] = 116 mg/L [8.0–17.0] versus 64 mg/L [3.8–11.2], $P = 0.001$), but the T-bil values were not significantly different (median [IQR] = 1.6 mg/dL [0.8–2.4] versus 1.8 mg/dL [0.8–2.7]) between semi-immune and non-immune patients.

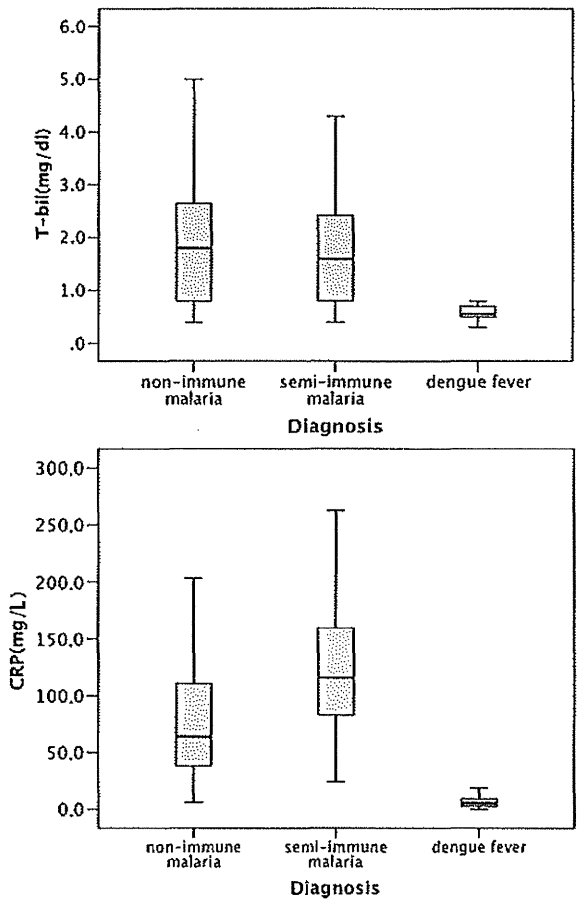

FIGURE 2. C-reactive protein (CRP) and total bilirubin (T-bil) values in patients with non-immune malaria, semi- immune malaria, and dengue fever. Non-immune malaria patients include 60 patients from non-endemic areas; semi-immune malaria patients include 26 patients from malaria endemic areas.

In both semi-immune and non-immune malaria groups, CRP and T-bil values were significantly higher than those values of the DF patients group ($P < 0.001$) (Figure 2).

DISCUSSION

Clinical histories, physical examination findings, and laboratory findings, such as anemia, help diagnose malaria. However, because the clinical manifestations of DF and malaria are similar, it is challenging to diagnose DF or malaria in travelers returning from regions where both DF and malaria are endemic, such as southeast Asia, south Asia, sub-Saharan Africa, Oceania, Latin America, and the Caribbean. Similarly, specific diagnostic tests are necessary for diagnosis, but they are not always available. It is important to distinguish between DF and malaria, because malaria can be fatal if treatment is delayed. Except for severe dengue, DF is generally a self-limiting disease. Our study suggests that CRP and T-bil are useful for distinguishing between DF and malaria in returned travelers.

In our study, differences in laboratory findings of DF and malaria were found in WBC, Ht, Plt, T-bil, LDH, and CRP values. In addition, CRP and T-bil had high AUCs of ROC curves (≥ 0.9). We found that CRP and T-bil are useful for distinguishing between DF and malaria.

Leukopenia, caused by bone marrow suppression by the dengue virus, is a common finding and a useful diagnostic feature for DF.[4,5] Thrombocytopenia, however, has been observed in both DF and malaria patients.[4,6] In our study, Plt levels were lower in malaria patients than dengue patients at the first presentation. In DF, Plt levels have been reported to be lowest 3–6 days from onset when the fever is about to resolve.[7] Therefore, because DF patients without fever were excluded in our study, Plt levels were lower in malaria patients than DF patients. Taylor and others[8] reported that Plt levels were a diagnostic finding for malaria; however, it is not useful to distinguish between DF and malaria, because thrombocytopenia is a characteristic finding in both diseases. Anemia caused by hemolysis of parasitized red blood cells increased splenic sequestration, and clearance of erythrocytes is common in malaria patients. Kain and others[6] reported that, in their study population of Canadian travelers, 41% of the patients diagnosed with malaria presented with anemia. Our study found that 32.6% of malaria patients had anemia at the first presentation. However, increased Ht levels are often observed because of hemoconcentration. In our study, the value of Ht in DF patients was significantly higher than the value in malaria patients, but it was not found to be useful for distinguishing between DF and malaria. In addition to

anemia, increased LDH levels from hemolysis of parasitized red blood cells were also observed in malaria patients.

Jaundice and an increase of T-bil levels are frequently observed in patients with severe malaria,[9] but they are rarely observed in DF. Taylor and others[8] reported that hyperbilirubinemia is the most diagnostic finding for malaria, with sensitivity of 38% and specificity of 95% in returning travelers. Our study results are in accordance with this report; we found that the increase in T-bil is a distinguishing laboratory finding in malaria patients compared with DF patients. CRP is an acute phase reactant, and markedly elevated levels of CRP are strongly associated with infection. Levels of CRP may also be elevated in patients with viral infections, although generally not to the degree seen in patients with bacterial infections.[10,11] Simon and others[11] evaluated the accuracy of determination of CRP levels for differentiating bacterial infections from viral fever and reported a sensitivity and specificity of 86% (95% CI = 65–95%) and 70% (95% CI = 19–96%), respectively. CRP levels are also elevated in malaria patients and useful in assessing malaria severity and follow-up.[12–14] Premaratna and others[15] reported that CRP was useful to distinguish between DF with right iliac fossa pain and acute appendicitis. In their report, all 12 DF patients had a CRP level < 12 mg/L.

We hypothesized that CRP values should be different between semi-immune malaria patients and non-immune patients because of their different immunological responses to malaria. The CRP values of semi-immune patients were, indeed, significantly higher than the values of non-immune patients ($P < 0.001$). CRP is still useful in distinguishing malaria patients from dengue patients, despite the CRP differences between semi-immune and immune malaria patients. T-bil levels were not significantly different between the malaria groups (i.e., immune versus semi-immune), and the values in both groups were significantly higher than the values of the DF group.

Because malaria and DF rarely occur in developed countries, rapid and easy access to specific tests or rapid diagnostic tests for malaria and DF are available only in limited hospitals and/or clinic settings. Giemsa stains are available in many hospital laboratories; however, few laboratory technicians have been trained to identify these diseases, thereby greatly decreasing the sensitivity and specificity of Giemsa stains for the diagnosis of malaria. Our study suggests that combining Giemsa stain results with CRP/T-bil values would enable physicians to differentiate malaria from dengue in returned travelers from endemic areas. Negative Giemsa stain and lower CRP and T-bil values would indicate DF rather than malaria.

In resource-limited settings, specific diagnostic tests, such as rapid diagnostic tests, are expensive; therefore, many cases of malaria are diagnosed without laboratory tests in endemic regions.[16] Such overtreatment of malaria has been tolerated in the era of inexpensive and safe monotherapy. However, with the introduction of artemisinin-based combination therapy (ACT), presumptive treatment becomes economically and clinically less acceptable. The test for CRP is an inexpensive laboratory test[17] compared with rapid diagnostic tests, and physicians can perform these tests without experienced laboratory technicians.

Our study has some limitations. We compared laboratory findings only in DF and malaria patients. According to GeoSentinel Surveillance during 2007–2011, DF and malaria cover 42.5% of febrile illness in returned travelers; this study does not include other febrile illnesses, such as typhoid fever, traveler's diarrhea, viral hepatitis, and schistosomiasis. The results of this study may not be applicable to all returning travelers. Additional prospective studies are needed to prove that CRP and T-bil are useful for diagnosis in all febrile patients returning from tropical regions.

Another limitation of our study is that we could not evaluate the usefulness of CRP and T-bil in severe DF or dengue hemorrhagic fever (DHF)/dengue shock syndrome (DSS) patients, because there were no severe DF or DHF/DSS patients included in this study. The enrollment criteria used in this study (i.e., febrile patients) might have contributed to excluding severe DF and DHF/DSS cases; vascular permeability of severe DF or DHF/DSS patients usually increases on days 3–7 when defervescence occurs.

In conclusion, CRP and T-bil are useful for distinguishing between DF and malaria in returning travelers. Lower CRP and T-bil values suggest DF, whereas higher values suggest malaria. These parameters may be helpful for diagnosis in hospitals where specific diagnostic tests are not available and resources are limited.

Received September 17, 2013. Accepted for publication December 5, 2013.

Published online January 13, 2014.

Financial support: This work was partly supported by funding from the Research on Emerging and Re-Emerging Infectious Diseases by the Ministry of Health, Labour, and Welfare, Japan (H23-shinkou-ippan-006).

Authors' addresses: Satoshi Kutsuna, Kayoko Hayakawa, Yasuyuki Kato, Yoshihiro Fujiya, Momoko Mawatari, Nozomi Takeshita, Shuzo Kanagawa, and Norio Ohmagari, National Center for Global Health and Medicine, Disease Control and Prevention Center, Toyko, Japan, E-mails: sonare.since1192@gmail.com, kayokohayakawa@gmail.com, katodcc@gmail.com, ilvtkfm@yahoo.co.jp, mawatamo@gmail.com, nozomitake@gmail.com, skanagaw@hosp.ncgm.go.jp, and lukenorioom@gmail.com.

REFERENCES

1. Leder K, Torresi J, Libman MD, Cramer JP, Castelli F, Schlagenhauf P, Wilder-Smith A, Wilson ME, Keystone JS, Schwartz E, Barnett ED, von Sonnenburg F, Brownstein JS, Cheng AC, Sotir MJ, Esposito DH, Freedman DO, 2013. GeoSentinel Surveillance Network. GeoSentinel surveillance of illness in returned travelers, 2007–2011. *Ann Intern Med 158:* 456–468.
2. Centers for Disease Control and Prevention (CDC), 2013. Ongoing dengue epidemic - Angola, June 2013. *MMWR Morb Mortal Wkly Rep 62:* 504–507.
3. Amarasinghe A, Kuritsk JN, Letson GW, Margolis HS, 2011. Dengue virus infection in Africa. *Emerg Infect Dis 17:* 1349–1354.
4. Potts JA, Rothman AL, 2008. Clinical and laboratory features that distinguish dengue from other febrile illnesses in endemic populations. *Trop Med Int Health 13:* 1328–1340.
5. Kalayanarooj S, Vaughn DW, Nimmannitya S, Green S, Suntayakorn S, Kunentrasai N, Viramitrachai W, Ratanachueke S, Kiatpolpoj S, Innis BL, Rothman AL, Nisalak A, Ennis FA, 1997. Early clinical and laboratory indicators of acute dengue illness. *J Infect Dis 176:* 313.
6. Kain KC, Harrington MA, Tennyson S, Keystone JS, 1998. Imported malaria: prospective analysis of problems in diagnosis and management. *Clin Infect Dis 27:* 142–149.
7. WHO, 2009. *WHO Guidelines Approved by the Guidelines Review Committee. Dengue: Guidelines for Diagnosis, Treatment, Prevention and Control: New Edition.* Geneva: World Health Organization.

8. Taylor SM, Molyneux ME, Simel DL, Meshnick SR, Juliano JJ, 2010. Does this patient have malaria? *JAMA 304:* 2048–2056.
9. Abro AH, Ustadi AM, Abro HA, Abdou AS, Younis NJ, Akaila SI, 2009. Jaundice with hepatic dysfunction in *P. falciparum* malaria. *J Coll Physicians Surg Pak 19:* 363–366.
10. Krüger S, Ewig S, Papassotiriou J, Kunde J, Marre R, von Baum H, Suttor N, Welte T; CAPNETZ Study Group, 2009. Inflammatory parameters predict etiologic patterns but do not allow for individual prediction of etiology in patients with CAP: results from the German competence network CAPNETZ. *Respir Res 10:* 65.
11. Simon L, Gauvin F, Amre DK, Saint-Louis P, Lacroix J, 2004. Serum procalcitonin and C-reactive protein levels as markers of bacterial infection: a systematic review and meta-analysis. *Clin Infect Dis 39:* 206.
12. Hurt N, Smith T, Tanner M, Mwankusye S, Bordmann G, Weiss NA, Teuscher T, 1994. Evaluation of C-reactive protein and haptoglobin as malaria episode markers in an area of high transmission in Africa. *Trans R Soc Trop Med Hyg 88:* 182–186.
13. Paul R, Sinha PK, Bhattacharya R, Banerjee AK, Raychaudhuri P, Mondal J, 2012. Study of C reactive protein as a prognostic marker in malaria from Eastern India. *Adv Biomed Res 1:* 41.
14. Gillespie SH, Dow C, Raynes JG, Behrens RH, Chiodini PL, McAdam KP, 1991. Measurement of acute phase proteins for assessing severity of *Plasmodium falciparum* malaria. *J Clin Pathol 44:* 228–231.
15. Premaratna R, Bailey MS, Ratnasena BG, de Silva HJ, 2007. Dengue fever mimicking acute appendicitis. *Trans R Soc Trop Med Hyg 101:* 683–685.
16. Amexo M, Tolhurst R, Barnish G, Bates I, 2004. Malaria misdiagnosis: effects on the poor and vulnerable. *Lancet 364:* 1896–1898.
17. National Collaborating Centre for Women's and Children's Health (United Kingdom), 2007. *Feverish Illness in Children: Assessment and Initial Management in Children Younger Than 5 Years. NICE Clinical Guidelines, No. 47.* London, UK: RCOG Press.

MAJOR ARTICLE

The First Identification and Retrospective Study of Severe Fever With Thrombocytopenia Syndrome in Japan

Toru Takahashi,[1,a] Ken Maeda,[4,a] Tadaki Suzuki,[6,a] Aki Ishido,[1] Toru Shigeoka,[1] Takayuki Tominaga,[1] Toshiaki Kamei,[2] Masahiro Honda,[3] Daisuke Ninomiya,[12] Takenori Sakai,[12] Takanori Senba,[12] Shozo Kaneyuki,[14] Shota Sakaguchi,[15] Akira Satoh,[16] Takanori Hosokawa,[18] Yojiro Kawabe,[19] Shintaro Kurihara,[17] Koichi Izumikawa,[17] Shigeru Kohno,[17] Taichi Azuma,[13] Koichiro Suemori,[13] Masaki Yasukawa,[13] Tetsuya Mizutani,[10] Tsutomu Omatsu,[10] Yukie Katayama,[10] Masaharu Miyahara,[20] Masahito Ijuin,[22] Kazuko Doi,[21] Masaru Okuda,[5] Kazunori Umeki,[11] Tomoya Saito,[11] Kazuko Fukushima,[11] Kensuke Nakajima,[11] Tomoki Yoshikawa,[7] Hideki Tani,[7] Shuetsu Fukushi,[7] Aiko Fukuma,[7] Momoko Ogata,[7] Masayuki Shimojima,[7] Noriko Nakajima,[6] Noriyo Nagata,[6] Harutaka Katano,[6] Hitomi Fukumoto,[6] Yuko Sato,[6] Hideki Hasegawa,[6] Takuya Yamagishi,[8] Kazunori Oishi,[8] Ichiro Kurane,[7] Shigeru Morikawa,[9] and Masayuki Saijo[7]

[1]Department of Hematology, [2]Department of Pathology, and [3]Emergency and Critical Care Medical Center, Yamaguchi Grand Medical Center, and [4]Laboratory of Veterinary Microbiology and [5]Laboratory of Veterinary Internal Medicine, Joint Faculty of Veterinary Medicine, Yamaguchi University, Yamaguchi, [6]Department of Pathology, [7]Department of Virology 1, [8]Infectious Disease Surveillance Center, and [9]Department of Veterinary Science, National Institute of Infectious Diseases, [10]Research and Education Center for Prevention of Global Infectious Diseases of Animals, Tokyo University of Agriculture and Technology, and [11]Tuberculosis and Infectious Disease Control Division, Ministry of Health, Labour and Welfare of Japan, Tokyo, [12]Department of Internal Medicine, Yawatahama City General Hospital, and [13]Department of Bioregulatory Medicine, Graduate School of Medicine, Ehime University, Ehime, [14]Department of Internal Medicine, Dohi Hospital, Hiroshima, [15]Department of Internal Medicine, Miyazaki Prefectural Nichinan Hospital, Miyazaki, [16]Section of Neurology, Nagasaki Kita Hospital, and [17]Department of Molecular Microbiology and Immunology, Graduate School of Biomedical Sciences, Nagasaki University, Nagasaki, [18]Department of Internal Medicine, Tosa Municipal Hospital, Kochi, and [19]Department of Rheumatology, Ureshino Medical Center, [20]Department of Hematology and [21]Department of Dermatology, Karatsu Red Cross Hospital, and [22]Community Medical Support Institute of Medicine, Saga University, Saga, Japan

(See the editorial commentary by Qiu and Kobinger on pages 811–2.)

Background. Severe fever with thrombocytopenia syndrome (SFTS) is caused by SFTS virus (SFTSV), a novel bunyavirus reported to be endemic in central and northeastern China. This article describes the first identified patient with SFTS and a retrospective study on SFTS in Japan.

Methods. Virologic and pathologic examinations were performed on the patient's samples. Laboratory diagnosis of SFTS was made by isolation/genome amplification and/or the detection of anti-SFTSV immunoglobulin G antibody in sera. Physicians were alerted to the initial diagnosis and asked whether they had previously treated patients with symptoms similar to those of SFTS.

Results. A female patient who died in 2012 received a diagnosis of SFTS. Ten additional patients with SFTS were then retrospectively identified. All patients were aged ≥50 years and lived in western Japan. Six cases were fatal. The ratio of males to females was 8:3. SFTSV was isolated from 8 patients. Phylogenetic analyses indicated that all of the Japanese SFTSV isolates formed a genotype independent to those from China. Most patients showed symptoms due to hemorrhage, possibly because of disseminated intravascular coagulation and/or hemophagocytosis.

Conclusions. SFTS has been endemic to Japan, and SFTSV has been circulating naturally within the country.

Keywords. Severe fever with thrombocytopenia syndrome; SFTS; SFTS virus: Japan; tick borne virus infection; bunyavirus; Hemophagocytosis.

Received 28 August 2013; accepted 26 September 2013; electronically published 14 November 2013.

[a]T. T., K. M., and T. S. contributed equally to this work.

Presented in part: 15th International Negative Strand Virus Meeting, Granada, Spain, 16–21 June 2013; Abstract 324.

Correspondence: Masayuki Saijo, MD, PhD, Department of Virology 1, National Institute of Infectious Diseases, Toyama 1-23-1, Shinjuku, Tokyo 162-8640, Japan msaijo@nih.go.jp).

The Journal of Infectious Diseases 2014;209:816–27

DOI: 10.1093/infdis/jit603

Severe fever with thrombocytopenia syndrome (SFTS), an infectious disease with a high case-fatality rate, is caused by SFTS virus (SFTSV), a novel bunyavirus reported to be endemic to central and northeastern parts of China [1, 2]. SFTSV, which is classified into the genus *Phlebovirus* and the family *Bunyaviridae*, is suspected to be a tick-borne virus owing to evidence of its presence in 2 species of ticks: *Haemaphysalis longicornis* and *Rhipicephalus microplus* [2, 3]. Approximately 2% of *H. longicornis* organisms collected from sheep, cattle, and dogs in Shandong Province tested positive for SFTSV in virus genome amplification assays [4]. A similar disease, which was named fever, thrombocytopenia and leukopenia syndrome (FTLS), was independently reported to be caused by a novel virus, Henan fever virus (HNFV) [1]. Despite the different names, "SFTS" and "FTLS" represent the same condition and "SFTSV" and "HNFV" represent the same virus. The case-fatality rate of SFTS is reported to be approximately 12% [1, 2]. Human-to-human transmission of SFTSV was reported to occur through close contact with the blood and/or body secretions of infected patients [5–9]. To our knowledge, there were no published reports of SFTS outside of China before we performed the study described here. Another tick-borne phlebovirus, the Heartland virus, which was detected in Missouri, is phylogenetically associated with SFTSV, caused severe febrile illness with thrombocytopenia, leukopenia in the total blood cell count, and elevated levels of liver enzymes [10].

We report the first identification of SFTS in Japan, which was detected in a previously healthy woman aged 50–59 years who died of multiple-organ failure in the autumn of 2012, and findings from a subsequent retrospective study of SFTS in Japan.

MATERIALS AND METHODS

Next-Generation Sequencing

Culture supernatants were subjected to viral RNA extraction using High Pure Viral Nucleic Acid Kit (Roche Diagnostics). Complementary DNA (cDNA) was synthesized using SuperScript III (Invitrogen) with random primers and then randomly amplified using the illustra GenomiPhi V2 Kit (GE Healthcare Life Sciences). A cDNA library was prepared using the Nextera DNA Sample Prep Kit (Illumina). A sequencing run for 50 nucleotides was performed with MiSeq (Illumina), using the MiSeq Reagent sequencing kit (Illumina). The assembled nucleotide sequences were used to determine homologous sequences by tBlast at the National Center for Biotechnology Information Web site (available at: http://blast.ncbi.nlm.nih.gov/Blast.cgi).

Viral Genome Detection, Virus Isolation, and Antibody Detection in Sera

The SFTSV genome was detected by reverse-transcription polymerase chain reaction (RT-PCR) in total RNA extracted from patient sera, using a High Pure Viral RNA kit (Roche Applied Science). Reverse transcription was performed with Ready-to-Go RT-PCR beads (GE Healthcare), using random nucleotide hexamers. PCR was performed to amplify SFTSV-specific cDNA fragments. PCR primer sets were designed to amplify the nucleoprotein (NP) region of the SFTSV genome (Supplementary Table 1). The PCR conditions were as follows: 1 cycle at 55°C for 30 minutes followed by 95°C for 2 minutes; 45 cycles at 94°C for 30 seconds, 52°C for 30 seconds, and 68°C for 30 seconds; followed by 1 cycle at 68°C for 5 minutes.

Vero cells were inoculated with RT-PCR–positive patient sera for virus isolation, cultured for 4–7 days, and examined for SFTSV antigen detection by indirect immunofluorescence assay (IFA) with a polyclonal antibody raised against SFTSV recombinant NP (rNP; rabbit anti-SFTSV rNP serum), which was produced as follows. SFTSV rNP tagged with histidine-tag on the C-terminus was expressed in a baculovirus expression system, as previously described [11, 12]. The NP gene of SFTSV strain HB29 (GenBank accession no. NC_018137) was artificially synthesized. Anti-SFTSV rNP serum was raised in rabbits by immunization with the purified SFTSV rNP, as previously described [13–15].

The neutralizing antibody to SFTSV Chinese isolate HB29 strain [2, 16] and Japanese isolate YG1 (this study) was detected as reported previously, except for the target virus [15]. With the exception of the antigen preparation, immunoglobulin G (IgG) antibody titers to SFTSV were determined by indirect IFA, using SFTSV HB29–infecting Vero cells as previously described [14].

Pathologic Studies With Histopathologic, Immunohistochemical, and In Situ Hybridization AT-Tailing (ISH-AT) Methods

Histopathologic studies of formalin-fixed and paraffin-embedded specimens were performed using hematoxylin-eosin stain.

Immunohistochemical analysis was performed as previously described, with some modifications [17]. The rabbit anti-SFTSV rNP serum and the peroxidase-labeled, polymer-conjugated anti-rabbit immunoglobulin (EnVision/HRP, Dako) were used in the immunohistochemical analysis as the primary and the secondary antibodies, respectively. Normal rabbit serum and lymph nodes of necrotizing lymphadenitis without SFTSV infection were used as negative controls for the antibody and tissue specimens, respectively.

ISH-AT was used for detection of SFTSV genomic RNA (negative-strand RNA) as reported previously, with the exception of the strand-specific oligonucleotide probes [18–20], which were designed for the S and L segments of the SFTSV genome (Supplementary Table 1).

Quantitative Amplification of the SFTSV Genome in the Autopsied Tissues and Organs

The SFTSV copy number was determined by performing quantitative real-time RT-PCR analysis of RNA samples extracted from paraffin-embedded sections as previously described, with

some modifications [17]. The amount of human β-actin messenger RNA (mRNA) in the DNase-treated RNA extracted from each section was also determined and used as an internal reference for normalization [21]. The primers and labeled probes are shown (Supplementary Table 1).

Electron Microscopic Analysis

The culture supernatant from Vero cells inoculated with SFTSV isolated from the first patient was used for electron microscopic analysis. The samples were fixed with 4% glutaraldehyde. The fixed samples were negatively stained with 2% phosphotungstic acid and then observed using a JEM-1400 transmission electron microscope (JEOL, Tokyo, Japan).

Recruitment of Patients With Suspected SFTS

The first diagnosis of SFTS in Japan was made public through an announcement from the Ministry of Health, Labor, and Welfare of Japan on 30 January 2013. Physicians were asked to volunteer information if they had treated patients who satisfied the following case definition: (1) fever of >38°C; (2) gastrointestinal tract symptoms, such as nausea, vomiting, abdominal pain, diarrhea, and melena; (3) thrombocytopenia, with $<100 \times 10^9$ platelets/L; (4) leukopenia, with $<4 \times 10^9$ white blood cells/L; (5) elevated levels of aspartate aminotransferase, alanine aminotransferase, and lactate dehydrogenase; (6) absence of other causes; and (7) death or admission to an intensive care unit because of the severity symptoms. Information about patients was collected from their physicians. The retrospective recruitment of patients with suspected SFTS was conducted from 30 January to 31 March 2013. Written informed consent was obtained from patients or responsible relatives.

Serum samples, which had been collected from the patients for future analyses to clarify the etiology and had been stored in each hospital by the respective physicians, used for the present study were sent to the Department of Virology 1 at the National Institute of Infectious Diseases (NIID; Tokyo, Japan) for virologic analyses. Clinical and laboratory data of the patients with SFTS were also sent to the corresponding author (M. Saijo) without information that made it possible to identify individuals.

Phylogenetic Analysis

cDNAs prepared from the patients' sera samples were used to determine SFTSV genome sequences. The terminal sequences of SFTSV genomes were determined by rapid amplification of cDNA ends (RACE) at the 3′ and 5′ ends, performed by RT-PCR after 3′ and 5′ linker ligation using a DynaExpress miRNA Cloning Kit, High Efficient (BioDynamics Laboratory, Tokyo, Japan). Purified RNA from the culture supernatant of SFTSV (YG1)–infected Vero cells was subjected to the 3′ linker ligation according to the manufacturer's protocol. Next, the 5′ linker was ligated to the 5′-phosphate end of the purified 3′ linker ligated RNA, according to the manufacturer's protocol, following RNA purification by NucleoSpin RNA Clean-up XS (Takara Bio, Shiga, Japan). The 3′ and 5′ linker ligated RNA was then reverse transcribed according to the manufacturer's protocol by SuperScript III (Invitrogen, Carlsbad, CA), using either the 3′ forward RT primer, which is the antiparallel sequence of the 3′ linker sequence, or the pd(N)6 primer (random hexamer). RT-PCR was performed using Q5 Hot Start High-Fidelity DNA Polymerase (NEB, Ipswich, MA) and SFTSV gene-specific primers (Supplementary Table 1) with the 3′ RT primer or the 5′ primer, which is the antiparallel sequence of the 5′ linker sequence.

Nucleotide sequences of each full segment of SFTSV in patients' sera were aligned using MUSCLE, an en suite program in the Molecular Evolutionary Genetics Analysis 5.1 software (MEGA Team, Japan). Evolutionary distances were estimated using Kimura's 2-parameter method, and phylogenetic trees were constructed using the neighbor-joining method. The robustness of the trees was tested using 1000 bootstrap replications. Accession numbers of the nucleotide sequences of SFTSV L-, M-, and S-segments are described in Supplementary Table 2.

Ethics Statement

Serum samples were used for virologic analysis after obtaining written informed consent from the patients themselves (for those who survived) or their responsible family members (for those who died). The clinical and laboratory data of the patients with SFTS were sent to the corresponding author without personally identifying information. All of the protocols and procedures were approved by the research and ethics committees of the NIID.

The polyclonal antibody to SFTSV rNP was produced by immunizing rabbits with purified SFTSV rNP, with approval from the Institutional Animal Care and Use Committee of the NIID (no. 111 124).

RESULTS

The First Patient in Japan Who Received a Diagnosis of SFTS

A previously healthy woman aged 50–59 years who lived in the Yamaguchi prefecture of Japan was hospitalized with high fever, fatigue, vomiting, and melena in the autumn of 2012. Her body temperature was 39.2°C. Tick bite wounds were not observed anywhere on her skin. Laboratory tests revealed a low platelet count of 89×10^9 platelets/L (normal range, 150–250×10^9 platelets/L) and a low white blood cell count of 0.4×10^9 cells/L (normal range, 4.0–8.0×10^9 cells/L). Serum levels of alanine aminotransferase, aspartate aminotransferase, and creatine kinase were abnormally high, while the C-reactive protein level was normal. A coagulation study revealed a prolonged activated partial thromboplastin time and a high D-dimer level. The patient's serum ferritin level of >40 000 μg/L was extremely elevated (normal range, 3–166 μg/L). Urinary analysis showed proteinuria and microhematuria. The blood culture was sterile. Computed tomography of the chest and

abdomen showed right axillary lymphadenopathy and bilateral renal swelling; however, there was no evidence of hepatosplenomegaly. Bone marrow aspiration revealed mildly hypocellular marrow with an increase in levels of activated histiocytes and hemophagocytes. The patient's condition deteriorated rapidly on the day following admission with the appearance of macrohematuria and a massive amount of tarry stool. Death occurred on the third day of hospitalization.

Serum was used for virus isolation using Vero and *Felis catus* whole fetus (Fcwf-4) cells. Cytopathic effect appeared in both cells within 5 days. Many DNA fragments that were homologous to those of SFTSV were detected in the culture supernatant of the cells inoculated in next-generation sequencing.

DNA amplified by conventional RT-PCR using either of 2 primer pairs showed the expected sizes of 458 or 461 bp in agarose-electrophoresis (data not shown). The inoculated Vero cells were tested for the presence of SFTSV antigen in indirect IFA with rabbit anti-SFTSV rNP serum and showed a similar positive reactivity (Figure 1*A*). Enveloped and spherical virions with approximate diameters of 100 nm were detected by electron microscopy (Figure 1*B*). The morphology of the virion is compatible with that of a bunyavirus. The virus isolated from the patient was named SFTSV YG1.

Autopsy findings included right axillary lymphadenopathy (3.5 × 2.0 cm; Figure 2*A*), bilateral renal swelling, mild retention of pericardial fluid (140 mL), and hepatic steatosis. Gastric ulceration was also observed in the pyloric region.

Severe necrotizing lymphadenitis with massive necrosis, the depletion of small lymphocytes, and severe infiltration of the swollen right axillary and right cervical lymph nodes by histiocytes and immunoblasts were observed (Figure 2*B* and 2*C*). Necrosis, which comprised nuclear debris and eosinophilic ghosts but not granulocytes, was distributed throughout the cortical area, the sinuses, and the capsule of the lymph node and had spread to the perinodal adipose tissue. No clusters of epithelioid histiocytes, stellate microabscesses, or granulomas were observed. There were no obvious intranuclear or intracytoplasmic viral inclusions. Prominent hemophagocytosis was observed in these lymph nodes, the bone marrow, and the spleen (Figure 2*D* and 2*E*). The bone marrow was relatively hypocellular, with no reduction in the number of megakaryocytes. The liver showed mild microvesicular fatty changes in zone 3 and mild inflammation, comprising lymphocytes and macrophages, around the portal tracts. The kidney showed subepithelial hemorrhage within the renal pelvis (Figure 2*F*). Significant hemophagocytosis were also observed in the mediastinal, hilar, and abdominal lymph nodes with no evidence of necrosis (Figure 3*A*, 3*C*, and 3*E*). The findings in the remaining visceral organs were unremarkable.

Positive signals for SFTSV NP antigen were detected in the cytoplasm of blastic cells and necrotic regions in the cortical area of the right axillary lymph node (Figure 3*B*). Viral antigen-positive cells were also detected in the right cervical lymph nodes (Figure 3*D*) but not in the mediastinal lymph nodes (Figure 3*F*), regardless of the level of immunoblast infiltration and hemophagocytosis (Figure 3*E*). Relatively few SFTSV antigen–positive cells were detected in the bone marrow, adrenal glands, the liver, and the spleen (Figure 3*G–J*), with no notable cytopathic effects or necrosis. No antigen-positive cells were detected in the heart, lungs, kidneys, gastrointestinal tract, aorta, or iliopsoas muscle.

The SFTSV genome, SFTSV genomic RNA (negative-strand RNA; Figure 4*A*), and mRNA (positive-strand RNA; Figure 4*B*) were detected in the blastic cells in the right cervical lymph node by ISH-AT analysis [18–20], while no signals were detected using an irrelevant probe as a negative control (Figure 4C). No signals showing necrotizing lymphadenitis without SFTSV infection were detected in the lymph nodes (negative control; Figure 4*D*).

SFTSV RNA was present, with high copy numbers, in the right axillary and cervical lymph node sections (Supplementary Table 3). Consistent with immunohistochemical analysis results, low copy numbers (100–1000 copies) of SFTSV RNA were also detected in the bone marrow, the spleen, the liver, and the adrenal glands. A few copies (<100) were detected in other tissue sections that did not contain antigen-positive cells (as assessed by immunohistochemical analysis), suggesting that quantitative real-time RT-PCR detected cell-free circulating SFTSV; a high viral load in the serum is characteristic of SFTS infection [22]. The number of SFTSV RNA copies/cell was calculated using the β-actin mRNA copy number, estimated at 1500 copies/cell [17]. The SFTSV RNA copy numbers in the right axillary and cervical lymph node sections were the highest among the tissues tested, while the bone marrow, spleen, and liver showed relatively lower copy numbers per cell (Supplementary Table 3).

The Retrospective Study

Serum samples collected from 23 patients who were retrospectively suspected of having SFTS were sent to the Department of Virology 1, NIID (Figure 5). The male-to-female ratio was 18:5. The earliest infection dated back to 2005 (Figure 5*B*). Serum samples collected from 21 patients (for 2 patients, acute phase serum samples were not available for virologic analysis) were subjected to virus isolation and RT-PCR for amplification of the SFTSV genome. Serum samples collected from all 23 patients were tested for IgG and immunoglobulin M (IgM) antibodies to SFTSV in the indirect IFA. Of the 23 patients, 8 men and 2 women received a diagnosis of SFTS: 7 had positive results of virus isolation and genome amplification tests; 1 had positive results of virus genome amplification testing and IgM antibody to SFTSV but had negative results of virus isolation analysis; and 2 were positive for IgG antibody to SFTSV. In the present study, the 2 patients who tested positive for SFTSV on the basis of detection of IgG to SFVSV were regarded as SFTS

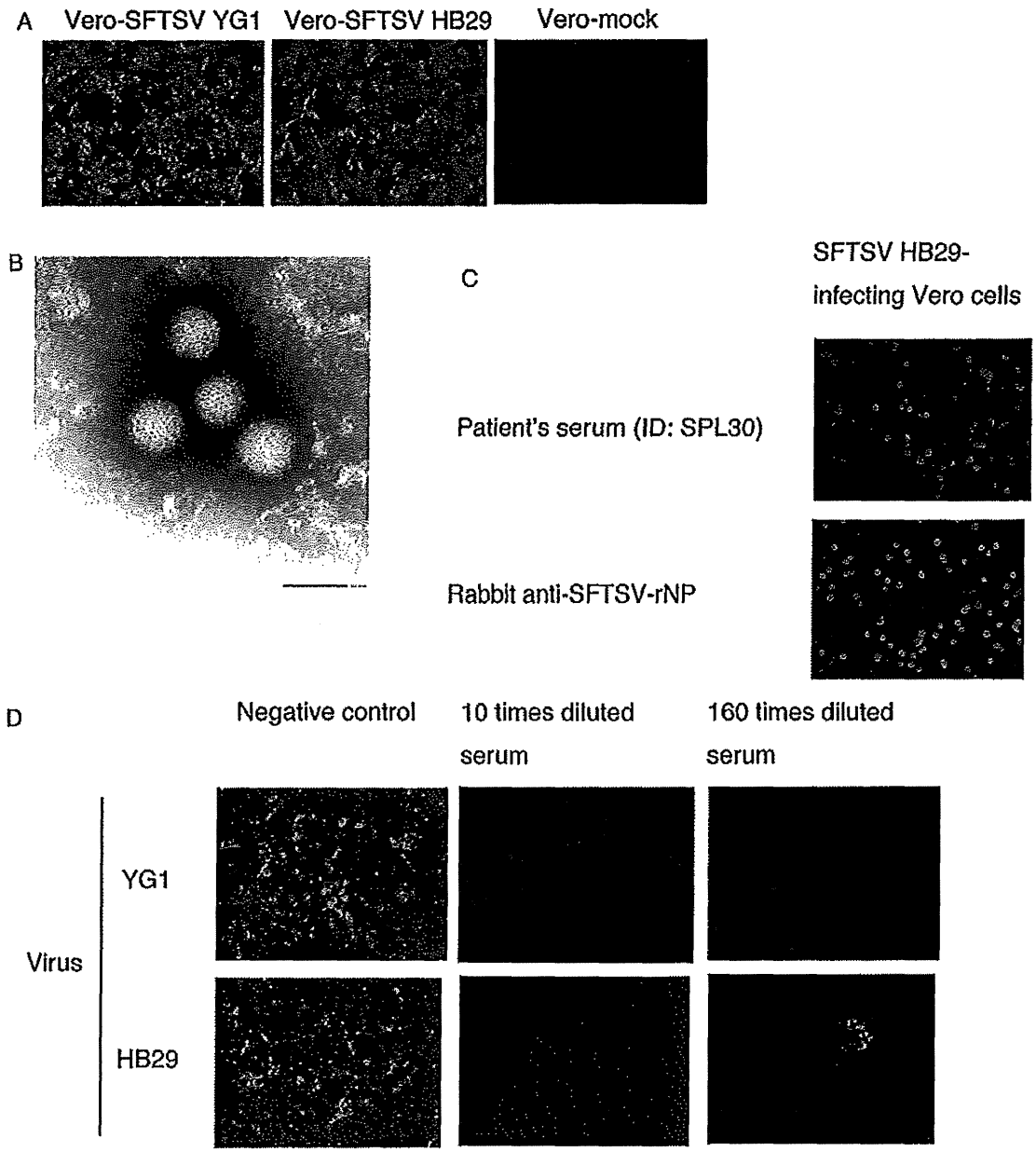

Figure 1. Reactivity of patient sera samples to severe fever with thrombocytopenia syndrome virus (SFTSV). *A*, Detection of SFTSV antigen in Vero cells by indirect immunofluorescence assay (IFA) with rabbit anti-SFTSV recombinant nucleoprotein (rNP) serum. *B*, Virions in the culture supernatant detected by electron microscopy (bar in the image indicates the length of 100 nm, ID: SPL004). *C*, Positive indirect IFA results of the serum collected from a surviving patient (ID: SPL030) in the convalescent phase of SFTSV HB29. *D*, Neutralizing antibody activity was induced in the serum collected from a patient (ID: SPL032) in the convalescent phase of SFTSV YG1 and SFTSV HB29.

positive because their symptoms were reminiscent of SFTS and because reports of asymptomatic cases in China are quite rare [23, 24]. For the purposes of the present study, the first patient was included with the 10 retrospective cases, for a total of 11 diagnosed cases.

All of the 11 patients in whom SFTS was diagnosed were aged ≥50 years (Figure 5*A*) and came from western Japan (Figure 5*D*). Disease onset occurred in all patients between the months of April and December (Figure 5*C*). Six of the 11 cases were fatal. There was clear evidence of tick bite in 2 cases.

Clinical Manifestation of 11 SFTS Patients

The clinical manifestations observed in SFTS patients are summarized in Table 1. All patients showed nonspecific febrile

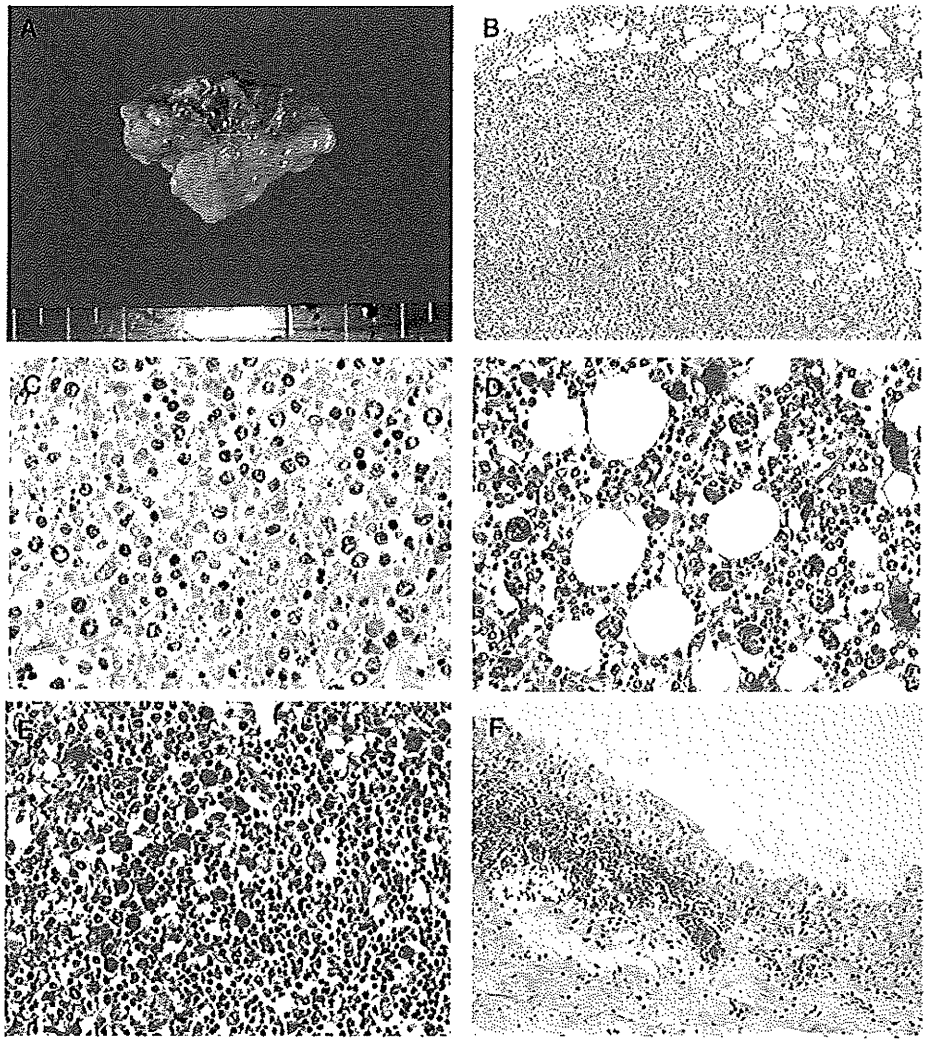

Figure 2. Macroscopic and microscopic findings under hematoxylin-eosin staining. *A*, Gross appearance of the swollen right axillary lymph node (3.5 × 2.0 cm). *B* and *C*, Microscopic findings in the right axillary lymph node. The basic architecture of the lymph node has been replaced by massive necrosis. The necrotic regions contain histiocytes, immunoblasts, nuclear debris, and eosinophilic ghosts but no neutrophils. *D* and *E*, Marked erythrophagocytosis in the bone marrow (*D*) and spleen (*E*). *F*, Acute subepithelial hemorrhage in the renal pelvis.

symptoms with gastrointestinal tract symptoms in the early phase of the disease. Deterioration in consciousness, characterized by dysarthria, disorientation, and alteration in consciousness, was commonly observed. Generalized convulsions were seen in the late stages of the disease in 5 of the 6 fatal cases. Respiratory symptoms were rarely observed. Superficial lymphadenopathy was detected in 5 patients.

Hemorrhagic symptoms such as petechiae, purpura, melena, bloody vomit, gingival bleeding as a form of discharge, and excessive bleeding at the site of skin biopsy were observed in 9 of the 11 patients.

Blood urea nitrogen and creatinine levels were elevated in 8 of 11 patients. Hematuria and proteinuria were observed in most patients.

In all 5 patients for whom bone marrow observation was performed, hemophagocytosis, with or without bone marrow cell dysplasia, was observed. The ferritin level was elevated in the blood of 8 patients, including the 5 in whom bone marrow examination was performed. Abnormalities were observed in tests in all of the patients for coagulopathy, prothrombin time, activated partial thromboplastin time, fibrin/fibrinogen degradation products, fibrinogen, and/or D-dimer.

Phylogenetic Analysis

The Japanese SFTSV strains were closely related to the SFTSV Chinese isolates but formed an independent cluster for each segment (Figure 6). No geographic or chronological relationship was found between the Japanese and Chinese strains.

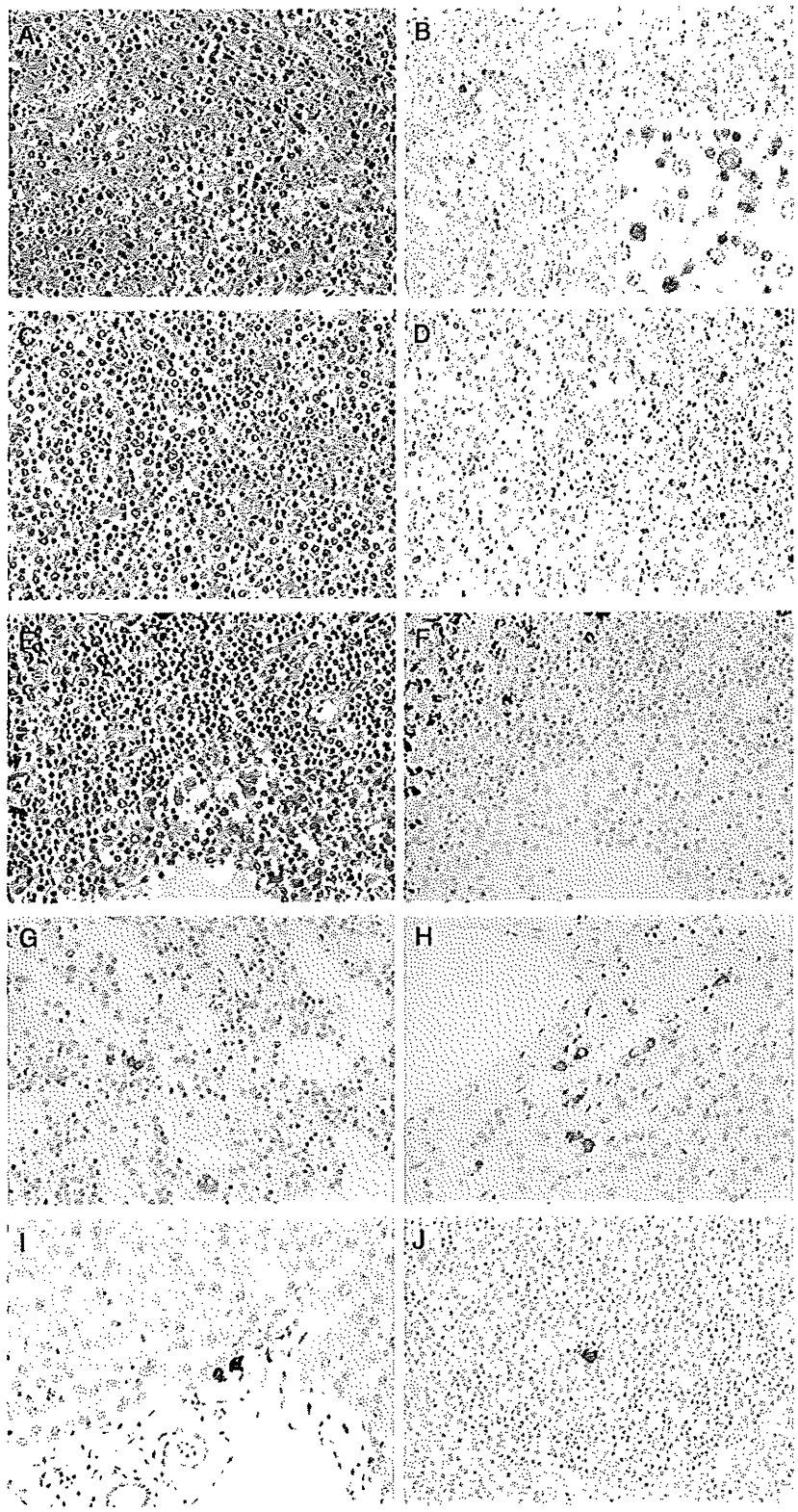

Figure 3. Microscopic and immunohistochemical tissue images. Hematoxylin-eosin staining (*A*, *C*, and *E*) and subsequent immunohistochemical analysis reveal the presence of severe fever with thrombocytopenia syndrome virus (SFTSV) NP (*B*, *D*, *F*, *G*, *H*, *I*, and *J*) in the right axillary (*A* and *B*), right cervical (*C* and *D*), and the mediastinal (*E* and *F*) lymph nodes. *A*, *C*, and *E*, Infiltration by immunoblasts and prominent hemophagocytosis was generally observed in the right axillary, right cervical, mediastinal, hilar, and abdominal lymph nodes; however, necrosis was only observed in the right axillary and cervical lymph nodes. *B*, *D*, and *F*, Viral antigen–positive cells were detected in the right axillary and cervical lymph nodes. Positive signals for SFTSV NP

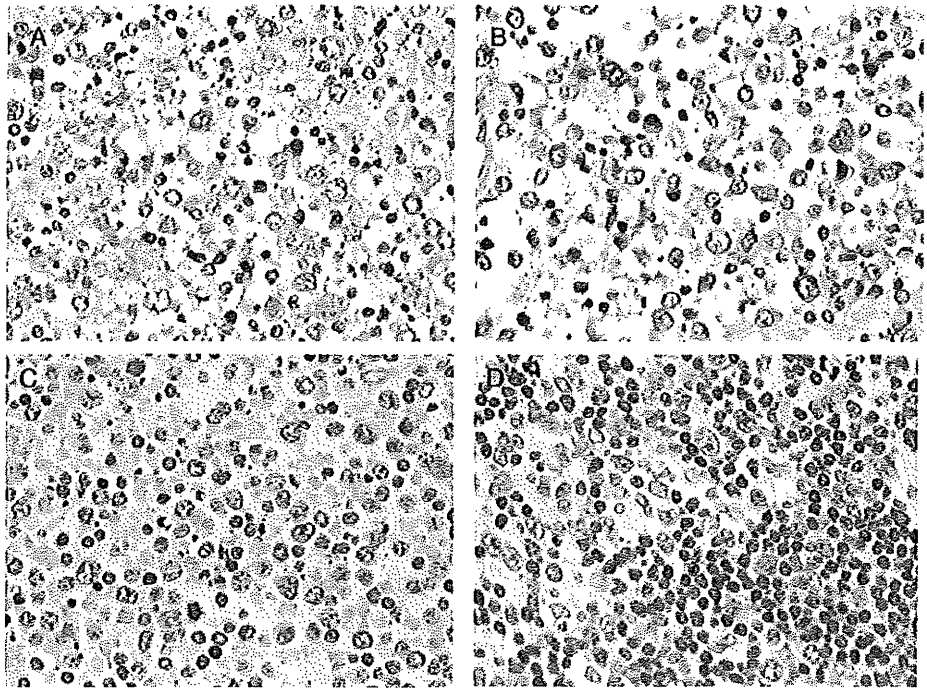

Figure 4. Detection of severe fever with thrombocytopenia syndrome virus (SFTSV) RNA in the right cervical lymph node by the in situ hybridization AT-tailing method. *A*, SFTSV genomic RNA was detected in the right cervical lymph node by the in situ hybridization AT-tailing method and a sense probe. SFTSV genomic RNA was detected in the cytoplasm of the blastic cells. *B*, The in situ hybridization AT-tailing method with an anti-sense probe detected a few cells in the right cervical lymph node that were positive for SFTSV messenger RNA (mRNA). SFTSV mRNA was also detected in the cytoplasm of blastic cells. *C*, No signals were detected in the right axillary lymph node by the in situ hybridization AT-tailing method with an irrelevant probe (negative control). *D*, A SFTSV sense probe detected no signals in lymph node sections showing necrotizing lymphadenitis without SFTSV infection.

Neutralizing Antibody Response to SFTSV

Sera collected from the 5 surviving patients with SFTS in the convalescent phase showed neutralizing activities to SFTSV Japanese isolate YG1 (Figure 1*D*). The sera of these 5 patients also showed similar degrees of neutralizing activities to SFTSV HB29.

DISCUSSION

The clinical manifestations of Japanese SFTS were very similar to those of severe cases of Chinese SFTS [1, 2], but the case-fatality rate (6 of 11 patients [55%]) was apparently higher than that in China, where an average of 12% of cases were fatal. It is worth noting that the characteristics of Japanese SFTS presented in this study were based on a limited number of patients and a strict case definition.

To our knowledge, this may be the first report describing the pathologic findings of a patient with SFTS. The local lymph nodes, which were the primary target organ in the first patient, served as the site of virus replication and showed marked pathologic changes, including massive necrosis. No neutrophil infiltration was observed in the patient. The spleen, liver, adrenal glands, and bone marrow contained a few SFTSV-infected cells. However, no viral antigens were detected in hepatocytes or in the parenchymal cells of the adrenal glands. Viruses belonging to the *Bunyaviridae* family, which includes the Rift valley fever virus, Hantaan virus, and Heartland virus [10], infect monocytes/macrophages [25, 26]. These cells may control the spread (or containment) of viruses to cells within other organs. The pathologic and virologic observations suggest that SFTSV replicated in the blastic cells within the lymph nodes and that replication took place predominantly in the local lymph nodes, not in the major organs.

Macrophages with phagocytosis of bone marrow cells were observed in all of the patients in whom bone marrow

Figure 3 continued. antigen were detected in the cytoplasm of blastic cells (B; inset). Inset shows a higher magnification (40×). In contrast, no signals were detected in the mediastinal lymph nodes, regardless of immunoblast infiltration and hemophagocytosis. G, H, I, and J, Immunohistochemical analysis of SFTSV NP was performed in the bone marrow (G), adrenal glands (H), liver (I), and spleen (J). A few SFTSV antigen–positive cells were observed in these tissues, with no notable cytopathic effects or necrosis (magnification, 20×; inset, 40×).

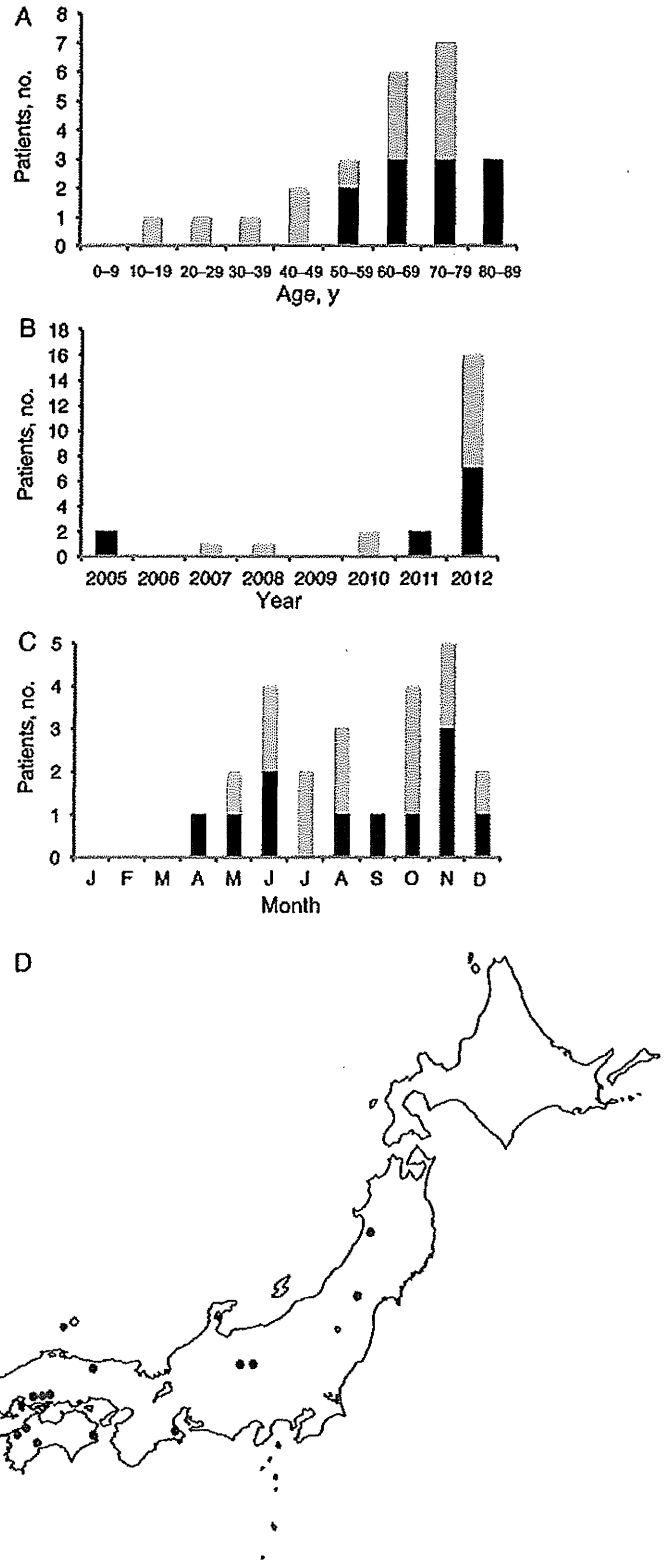

Figure 5. Chronological (*A*), age-based (*B*), geographic (*C*), and seasonal (*D*) distributions of patients with retrospectively diagnosed severe fever with thrombocytopenia syndrome (SFTS) in Japan. Black and gray bars in panels *A–C* indicate patients with and those without SFTS, respectively. The red and blue circles in panel *D* indicate the areas where patients with and those without SFTS were located.

Table 1. Summary of Clinical Manifestation of Retrospectively Diagnosed Japanese Severe Fever With Thrombocytopenia Syndrome Cases

Symptom or Laboratory Parameter	Variable (n = 11)
Clinical manifestation, positive/negative/unknown	
Fever	11/0/0
General symptoms	
General fatigue	11/0/0
Myalgia	2/5/4
Arthralgia	1/6/4
Headache	6/4/1
Gastrointestinal tract symptoms	
Overall	11/0/0
Nausea	9/2/0
Vomiting	6/5/0
Abdominal pain	6/5/0
Diarrhea	7/4/0
Anorexia	11/0/0
Respiratory symptoms	
Overall	3/8/0
Throat pain	2/9/0
Cough	1/10/0
Neurologic symptoms	
Overall	10/1/0
Dysarthria	3/8/0
Consciousness disturbance	8/3/0
Seizure	6/5/0
Hemorrhage	
Overall	9/2/0
Hemoptysis	1/10/0
Purpura	3/8/0
Bloody diarrhea	4/7/0
Gingival bleeding	5/6/0
Nasal hemorrhage	0/11/0
Genitourinary tract hemorrhage	0/11/0
Others	
Lymphadenopathy	5/6/0
Laboratory finding, no. (%)	
Total blood cell count	
Leukopenia	11 (100)
Thrombocytopenia	11 (100)
Serum chemistry	
Total protein level < 6.0 mg/dL (hypoproteinemia)	3 (27)
Albumin level < 3.0 mg/dL (hypoalbuminemia)	1 (9)
Aspartate aminotransferase level >30 IU/L	11 (100)
Alanine aminotransferase level >30 IU/L	11 (100)
Lactate dehydrogenase level >250 IU/L	11 (100)
Creatine kinase level >200 IU/L	11 (100)
Blood urea nitrogen level >20 mg/dL	7 (64)
Creatinine level >1 mg/dL	7 (64)
Inflammatory parameter	
C-reactive protein level >1 mg/dL	3 (27)
Urinalysis	
Hematuria	9 (90)[a]
Proteinuria	10 (100)[a]
Coagulopathy, no. (%)	
Abnormality in either DIC parameter[b]	11 (100)
Hemophagocytosis, no. (%)	
Bone marrow examination	
Hemophagocytosis	5 (100)[c]
Positive increased ferritin level	8 (100)[d]
Tick bite within 2 weeks of onset, no. (%)	2 (18)

[a] Basic number is 10.

[b] Disseminated intravascular coagulation (DIC) parameters include prothrombin time, activated partial thromboplastin time, and levels of antithrombin 3, fibrinogen, D-dimer, and fibrinogen degradation products.

[c] Basic number is 5.

[d] Basic number is 8.

examination was performed. Furthermore, pathologic examination of the lymph nodes, bone marrow, and the spleen of the initial patient revealed marked hemophagocytosis, regardless of the presence of SFTSV-infected cells (Figure 2*D* and 2*E* and Figure 3*A*, 3*C*, and 3*E*). Ferritin level was extremely elevated in the sera of all patients who were tested. Abnormality in coagulopathy-associated indices was also observed in all patients. SFTSV infections induced a cytokine storm, the level of which was associated with the severity of SFTS [27]. These results indicate that in addition to multiorgan dysfunction, hemophagocytosis and disseminated intravascular coagulation are major factors for poor prognosis.

The mode of the natural SFTSV lifecycle in Japan should be clarified to enable better identification of risk factors for SFTSV infection and to address strategies for reducing the risk of infections. Further study is necessary to clarify the circulation of SFTSV in nature in Japan, in terms of tick species, percentages of SFTSV positivity for each tick species, and the prevalence of SFTSV-positive ticks, to better determine and evaluate the risk factors for SFTSV infection in Japan.

Japanese isolates formed a cluster that was independent from Chinese isolates (Figure 6), indicating that SFTSV has been circulating in Japan naturally for some time. The earliest year for which we have evidence of SFTS in patient sera samples was 2005, and to our knowledge, the article by Liu et al, which concerns SFTS occurrence in China during 2006, reports the oldest cases from China [5]. It is also noteworthy that patients with SFTS were reported in South Korea in 2013

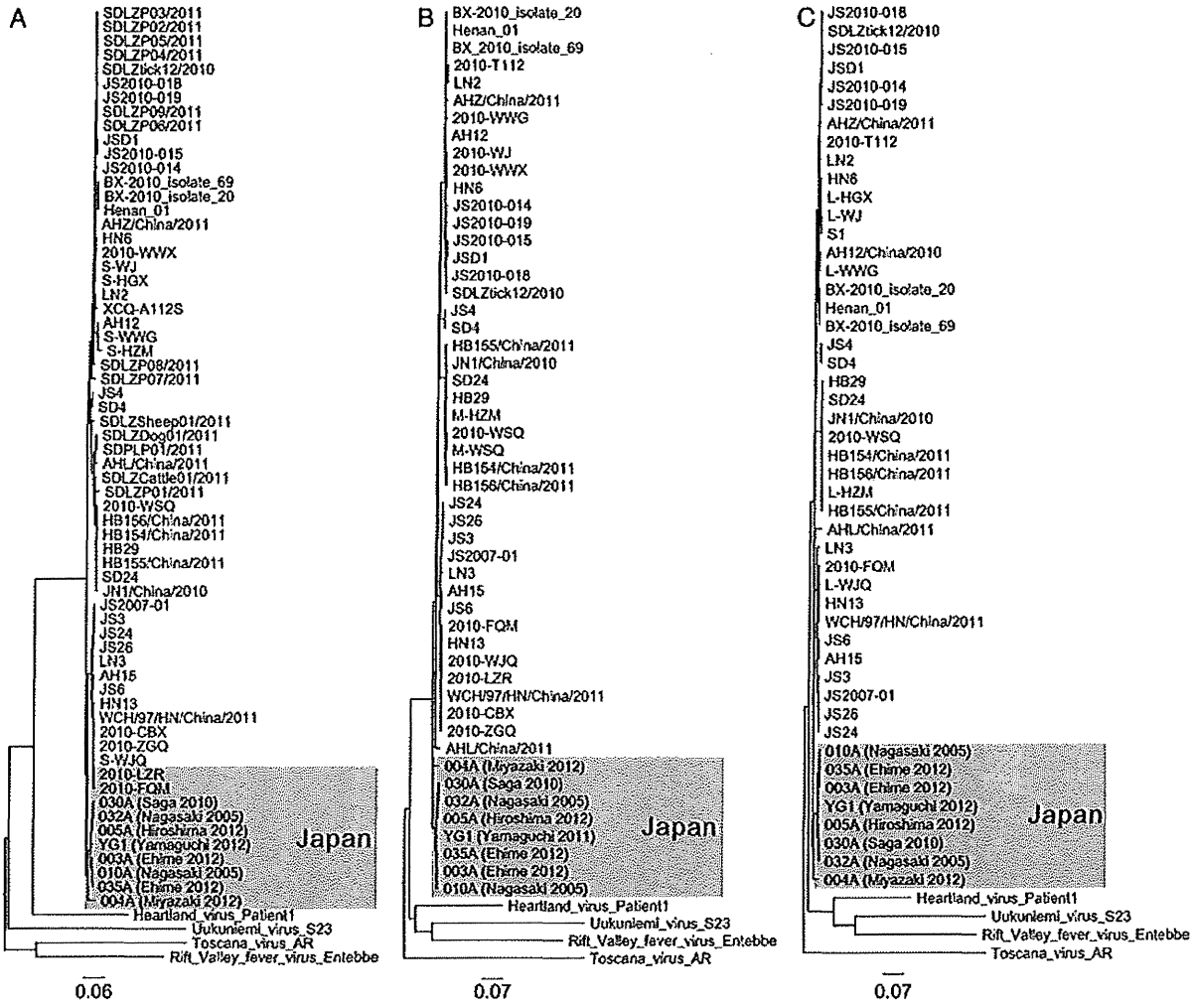

Figure 6. Phylogenetic trees showing the phylogenetic positions of severe fever with thrombocytopenia syndrome virus (SFTSV) strains in Japan, compared with other known strains. Trees are based on the S segment (*A*; left panel), M segment (*B*; middle panel), and L segment (*C*; right panel). Heartland virus, Uukuniemi virus, Toscana virus, and Rift Valley fever virus are included in the phylogenetic analyses.

(ProMed mail: archive numbers 20130521.1729124 and 20130529.174441). The prevalence of SFTS in and around East Asia should be studied to clarify the nature of SFTS in the region.

In conclusion, SFTSV is prevalent in Japan. Japanese SFTSV strains have characteristics similar to those of Chinese isolates but an independent genotype, which indicates that SFTSV has been present in Japan for some time.

Supplementary Data

Supplementary materials are available at *The Journal of Infectious Diseases* online (http://jid.oxfordjournals.org/). Supplementary materials consist of data provided by the author that are published to benefit the reader. The posted materials are not copyedited. The contents of all supplementary data are the sole responsibility of the authors. Questions or messages regarding errors should be addressed to the author.

Notes

Acknowledgments. We thank Dr De-Xin Li and Dr Mi-Fang Liang, National Institute for Viral Disease Control and Prevention, Chinese Center for Disease Control and Prevention, Beijing, PRC, for providing us with the SFTSV HB29 strain; Dr Roger Hewson, Virology, Pathogenesis, and Emerging Disease, Public Health England–Microbiology Services, Porton Down, Salisbury, United Kingdom, for his critical comments; and the municipal officials who supported this work, in the prefectures in which patients with SFTS were reported.

Financial support. This work was supported by the Ministry of Health, Labor and Welfare Science Research (grants in aid H24-Shinko-Ippan-013, H22-Shinko-Ippan-006, and H25-Shinko-Shitei-009).

Potential conflicts of interest. All authors: No reported conflicts.

All authors have submitted the ICMJE Form for Disclosure of Potential Conflicts of Interest. Conflicts that the editors consider relevant to the content of the manuscript have been disclosed.

References

1. Xu B, Liu L, Huang X, et al. Metagenomic analysis of fever, thrombocytopenia and leukopenia syndrome (FTLS) in Henan Province, China: discovery of a new bunyavirus. PLoS Pathog **2011**; 7:e1002369.
2. Yu XJ, Liang MF, Zhang SY, et al. Fever with thrombocytopenia associated with a novel bunyavirus in China. N Engl J Med **2011**; 364:1523–32.
3. Zhang YZ, Zhou DJ, Qin XC, et al. The ecology, genetic diversity, and phylogeny of Huaiyangshan virus in China. J Virol **2012**; 86:2864–8.
4. Jiang XL, Wang XJ, Li JD, et al. Isolation, identification and characterization of SFTS bunyavirus from ticks collected on the surface of domestic animals [in Chinese]. Chin J Virol **2012**; 28:252–7.
5. Liu Y, Li Q, Hu W, et al. Person-to-person transmission of severe fever with thrombocytopenia syndrome virus. Vector Borne Zoonotic Dis **2012**; 12:156–60.
6. Gai Z, Liang M, Zhang Y, et al. Person-to-person transmission of severe fever with thrombocytopenia syndrome bunyavirus through blood contact. Clin Infect Dis **2012**; 54:249–52.
7. Bao CJ, Guo XL, Qi X, et al. A family cluster of infections by a newly recognized bunyavirus in eastern China, 2007: further evidence of person-to-person transmission. Clin Infect Dis **2011**; 53:1208–14.
8. Chen H, Hu K, Zou J, Xiao J. A cluster of cases of human-to-human transmission caused by severe fever with thrombocytopenia syndrome bunyavirus. Int J Infect Dis **2013**; 17:e206–8.
9. Tang X, Wu W, Wang H, et al. Human-to-human transmission of severe fever with thrombocytopenia syndrome bunyavirus through contact with infectious blood. The J Infect Dis **2013**; 207:736–9.
10. McMullan LK, Folk SM, Kelly AJ, et al. A new phlebovirus associated with severe febrile illness in Missouri. New Engl J Med **2012**; 367:834–41.
11. Saijo M, Niikura M, Morikawa S, et al. Enzyme-linked immunosorbent assays for detection of antibodies to Ebola and Marburg viruses using recombinant nucleoproteins. J Clin Microbiol **2001**; 39:1–7.
12. Kitts PA, Possee RD. A method for producing recombinant baculovirus expression vectors at high frequency. BioTechniques **1993**; 14:810–7.
13. Saijo M, Qing T, Niikura M, et al. Recombinant nucleoprotein-based enzyme-linked immunosorbent assay for detection of immunoglobulin G antibodies to Crimean-Congo hemorrhagic fever virus. J Clin Microbiol **2002**; 40:1587–91.
14. Saijo M, Qing T, Niikura M, et al. Immunofluorescence technique using HeLa cells expressing recombinant nucleoprotein for detection of immunoglobulin G antibodies to Crimean-Congo hemorrhagic fever virus. J Clin Microbiol **2002**; 40:372–5.
15. Saijo M, Ogino T, Taguchi F, et al. Recombinant nucleocapsid protein-based IgG enzyme-linked immunosorbent assay for the serological diagnosis of SARS. J Virol Methods **2005**; 125:181–6.
16. Jin C, Liang M, Ning J, et al. Pathogenesis of emerging severe fever with thrombocytopenia syndrome virus in C57/BL6 mouse model. Proc Natl Acad Sci USA **2012**; 109:10053–8.
17. Nakajima N, Hata S, Sato Y, et al. The first autopsy case of pandemic influenza (A/H1N1pdm) virus infection in Japan: detection of a high copy number of the virus in type II alveolar epithelial cells by pathological and virological examination. Jpn J Infect Dis **2010**; 63:67–71.
18. Nakajima N, Ionescu P, Sato Y, et al. In situ hybridization AT-tailing with catalyzed signal amplification for sensitive and specific in situ detection of human immunodeficiency virus-1 mRNA in formalin-fixed and paraffin-embedded tissues. Am J Pathol **2003**; 162:381–9.
19. Nakajima N, Asahi-Ozaki Y, Nagata N, et al. SARS coronavirus-infected cells in lung detected by new in situ hybridization technique. Jpn J Infect Dis **2003**; 56:139–41.
20. Nakajima N, Sata T, Hanaki K, Kurata T, Yoshikura H. Application of the hybridization AT-tailing method for detection of human immunodeficiency virus RNA in cells and simian immunodeficiency virus RNA in formalin-fixed and paraffin-embedded tissues. J Virol Methods **1999**; 81:169–77.
21. Kuramochi H, Hayashi K, Uchida K, et al. Vascular endothelial growth factor messenger RNA expression level is preserved in liver metastases compared with corresponding primary colorectal cancer. Clin Cancer Res **2006**; 12:29–33.
22. Huang X, Liu L, Du Y, et al. Detection of a novel bunyavirus associated with fever, thrombocytopenia and leukopenia syndrome in Henan Province, China, using real-time reverse transcription PCR. J Med Microbiol **2013**; 62:1060–4.
23. Zhao L, Zhai S, Wen H, et al. Severe fever with thrombocytopenia syndrome virus, Shandong Province, China. Emerg Infect Dis **2012**; 18: 963–5.
24. Cui F, Cao HX, Wang L, et al. Clinical and epidemiological study on severe Fever with thrombocytopenia syndrome in yiyuan county, shandong province, china. Am J Trop Med Hyg **2013**; 88:510–2.
25. Lewis RM, Morrill JC, Jahrling PB, Cosgriff TM. Replication of hemorrhagic fever viruses in monocytic cells. Rev Infect Dis **1989**; 11(Suppl 4):S736–42.
26. Nagai T, Tanishita O, Takahashi Y, et al. Isolation of haemorrhagic fever with renal syndrome virus from leukocytes of rats and virus replication in cultures of rat and human macrophages. J Gen Virol **1985**; 66 (Pt 6):1271–8.
27. Sun Y, Jin C, Zhan F, et al. Host cytokine storm is associated with disease severity of severe fever with thrombocytopenia syndrome. J Infect Dis **2012**; 206:1085–94.

frontiers in
MICROBIOLOGY

REVIEW ARTICLE
published: 05 September 2013
doi: 10.3389/fmicb.2013.00267

Animal models for Ebola and Marburg virus infections

Eri Nakayama and Masayuki Saijo*

Department of Virology 1, National Institute of Infectious Diseases, Tokyo, Japan

Edited by:
Akio Adachi, The University of Tokushima Graduate School, Japan

Reviewed by:
Stefan Pöhlmann, German Primate Center, Germany
Takeo Ohsugi, Kumamoto University, Japan

****Correspondence:***
Masayuki Saijo, Department of Virology 1, National Institute of Infectious Diseases, Toyama 1-23-1, Shinjuku-ku, Tokyo 162-8640, Japan
e-mail: msaijo@nih.go.jp

Ebola and Marburg hemorrhagic fevers (EHF and MHF) are caused by the Filoviridae family, *Ebolavirus* and *Marburgvirus* (ebolavirus and marburgvirus), respectively. These severe diseases have high mortality rates in humans. Although EHF and MHF are endemic to sub-Saharan Africa. A novel filovirus, Lloviu virus, which is genetically distinct from ebolavirus and marburgvirus, was recently discovered in Spain where filoviral hemorrhagic fever had never been reported. The virulence of this virus has not been determined. Ebolavirus and marburgvirus are classified as biosafety level-4 (BSL-4) pathogens and Category A agents, for which the US government requires preparedness in case of bioterrorism. Therefore, preventive measures against these viral hemorrhagic fevers should be prepared, not only in disease-endemic regions, but also in disease-free countries. Diagnostics, vaccines, and therapeutics need to be developed, and therefore the establishment of animal models for EHF and MHF is invaluable. Several animal models have been developed for EHF and MHF using non-human primates (NHPs) and rodents, which are crucial to understand pathophysiology and to develop diagnostics, vaccines, and therapeutics. Rhesus and cynomolgus macaques are representative models of filovirus infection as they exhibit remarkably similar symptoms to those observed in humans. However, the NHP models have practical and ethical problems that limit their experimental use. Furthermore, there are no inbred and genetically manipulated strains of NHP. Rodent models such as mouse, guinea pig, and hamster, have also been developed. However, these rodent models require adaptation of the virus to produce lethal disease and do not mirror all symptoms of human filovirus infection. This review article provides an outline of the clinical features of EHF and MHF in animals, including humans, and discusses how the animal models have been developed to study pathophysiology, vaccines, and therapeutics.

Keywords: Ebola virus, Marburg virus, filovirus, animal models, viral hemorrhagic fever

INTRODUCTION

The Family *Filoviridae* includes three accepted genera, *Ebolavirus* (ebolavirus), *Marburgvirus* (marburgvirus), and *Cuevavirus* (**Figure 1**) (Kuhn et al., 2011, 2013). Filoviruses are classified as biosafety level 4 (BSL-4) agents because they cause severe hemorrhagic fevers in humans and non-human primates (NHPs) with high case-fatality rates, ranging between 23 and 90% (Sanchez et al., 2007). Each of the *Marburgvirus* and *Cuevavirus* genera consists of a single species, *Marburg marburgvirus* and *Lloviu cuevavirus*, respectively. The genus *Marburgvirus* has two subspecies: Marburg virus (MARV) and Ravn virus (RAVV). The genus *Ebolavirus* is divided into five distinct species, *Zaire ebolavirus* (Ebola virus, EBOV), *Sudan ebolavirus* (Sudan virus, SUDV), *Tai Forest ebolavirus* (Tai Forest virus, TAFV), *Bundibugyo ebolavirus* (Bundibugyo virus, BDBV), and *Reston ebolavirus* (Reston virus, RESTV; Kuhn et al., 2013). EBOV is highly virulent to humans and NHPs with a mortality rate of up to 90% in African epidemics. The case fatality rate of SUDV and BDBV is ~50 and 25%, respectively; the only person known to have been infected with TAFV survived. RESTV has been known to cause symptomatic disease in NHPs but not in humans. Lloviu virus belonging to the genus *Cuevavirus* was identified in the absence of replicating isolates during an investigation of die-off bats in Spain and the virulence for humans and NHPs has not been assessed (Negredo et al., 2011).

Although there has been an increasing frequency of filovirus outbreaks reported from endemic regions of Africa and Asia in recent years, there are no licensed vaccines or effective therapeutics for filovirus hemorrhagic fever.

The primary source of patients with filovirus hemorrhagic fever was mainly linked to exposure to animal carcasses found in the forest or to the putative bat reservoir, resulting in subsequent transmission through direct person-to-person contact (Leroy et al., 2004, 2009). Filoviruses enter the body via direct contact with infectious blood and/or body fluids. After an incubation period of 2–21 days, non-specific initial symptoms such as fever, chills, fatigue, headache, and myalgia appear. About 5–7 days after onset, a maculopapular rash usually develops on the face, buttocks, trunk, and/or arms and later generalizes over the entire body. As disease progresses, systemic (prostration, lethargy), gastrointestinal (anorexia, vomiting, abdominal pain, diarrhea), respiratory (chest pain, breath shortness, cough, nasal discharge), vascular (conjunctival injection, postural hypotension, edema), and neurological (headache, confusion, coma)

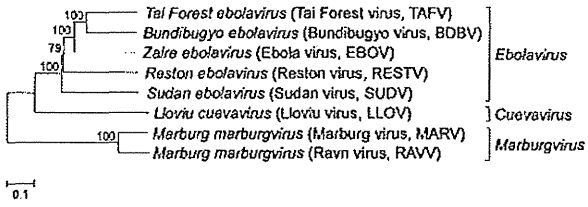

FIGURE 1 | Phylogenetic analysis of filovirus based on nucleotide sequence. The phylogenetic tree based on complete viral genome sequences was constructed by using the neighbor-joining method. Numbers at branch points indicate bootstrap values (1000 replicates). The GenBank accession numbers of Tai Forest virus (TAFV), Bundibugyo virus (BDBV), Ebola virus (EBOV), Reston virus (RESTV), Sudan virus (SUDV), Lloviu virus (LLOV), Marburg virus (MARV), and Ravn virus (RAVV) are FJ217162, FJ217161, AF086833, AB050936, AY729654, JF828358, DQ217792, and EF446131, respectively.

manifestations are observed. Some patients develop multiple foci of mucosal hemorrhage, which is especially evident in conjunctiva and gingiva together with bleeding from venipuncture sites. Hemorrhagic symptoms observed during the peak of the illness include petechiae, ecchymoses, epistaxis, mucosal hemorrhages, and/or visceral hemorrhagic effusions. In fatal cases, patients die with hypovolemic shock and multiple organ failure between Day 6 and 16.

Animal models of filovirus infection have been developed in mice, guinea pigs, hamsters, and NHPs (Connolly et al., 1999; Bente et al., 2009; Bradfute et al., 2012; Wahl-Jensen et al., 2012). The development of animal models that accurately reflect human disease is critical to understanding the pathogenesis of Ebola and Marburg hemorrhagic fevers (EHF and MHF, respectively), because filoviral outbreaks in humans are sporadic and there is limited clinical data and access to human tissue. Since the wild-type virus replicates to high titers in NHPs and the virus causes symptoms, including hemorrhage and shock, which are similar to those of patients with EHF and MHF, NHP models may be the most useful to evaluate the efficacy of candidate vaccines and treatment measures. However, small animal models are also needed for preliminary evaluation of vaccines and therapeutic interventions against filovirus diseases, because of the ethical and handling issues related to using NHPs.

Here, we summarize and discuss the animal models developed for the study of hemorrhagic fever caused by filoviruses.

MOUSE MODELS

In contrast to the development of the NHP and guinea pig models, as described in later sections, development of a mouse model of filovirus infection has been unsuccessful due to the fact that adult immunocompetent mice were resistant to wild-type filovirus infection. The intraperitoneal or intracerebral inoculation of newborn mice and 4-day-old suckling mice with non-mouse adapted EBOV was shown to cause lethal infections, but 8-day-old or older mice did not show any symptoms (Johnson et al., 1995; Bray, 2001). Serial passage of wild-type EBOV in suckling mice was needed for adaptation, in which the virus acquired lethal virulence to adult immunocompetent mice (Bray, 2001). Intraperitoneal inoculation of mouse-adapted EBOV with a 1–100 plaque forming unit (pfu) dose (30–3000 times the median lethal dose) caused lethal infection to 5-week-old BALB/c, C57BL/6 and ICR (CD-1) mice, but subcutaneous inoculation of the virus at a dose of 10^6 pfu did not cause symptomatic illness in 3-week-old adult mice (Bray, 2001). This phenomenon is not observed in NHP and guinea pig models, which are susceptible to wild-type EBOV infection through any route of inoculation. $CD8^+$ T cells and perforin, but not B cells and $CD4^+$ T cells, are required for resistance to subcutaneous inoculation of EBOV (Gupta et al., 2005). It is supposed that the presence of regional lymph nodes and/or Langerhans cells in the skin contributes to protection from filoviral subcutaneous infection via activation of $CD8^+$ cells, however, there are no reports to prove this hypothesis.

It has been shown that mouse-adapted filovirus is fatal over a broad range of ages in BALB/c mice. Infected mice became acutely ill with symptoms of ruffled fur, reduced activity, and weight loss on Day 3–4 post-infection and died on Days 5–7, although these lengths differed depending on the challenge dose (Bray et al., 1999; Warfield et al., 2009). Virus titer in the liver and spleen exceeded 10^7 pfu/g within 3 days after infection and then reached a maximum of over 10^9 pfu/g at Day 5 post-inoculation. These titers exceeded the peak viral concentrations in the liver and spleen of infected guinea pigs (about 10^6 pfu/g) and NHPs (about 10^7 pfu/g; Bray et al., 1999). The virus is generally undetectable in serum on Day 1, but by Day 3 the viremia level peaks at approximately 10^7 pfu/ml, which was comparable to that in NHPs and exceeds that in guinea pigs (10^{4-5} pfu/ml; Bray et al., 1999).

As seen in the NHP model, the systemic viral spread results in extensive infection and necrosis of the liver, spleen, and other organs (Bray et al., 1999; Warfield et al., 2009). In liver from mice infected with mouse-adapted EBOV or RAVV, viral replication was observed in hepatocytes, Kupffer cells, and sinusoidal endothelial lining cells. Histological lesions were observed by Day 4 after inoculation, including coalescing, foci of hepatocellular vacuolar change, degeneration, and necrosis of hepatocytes. In the spleen, viral antigen was detected on Day 2 after infection, at which point coagulopathy, such as disseminated intravascular coagulation (DIC) accompanied by prolongation of prothrombin time (PT) and activated partial thromboplastin time (aPTT), was not observed in the moribund mice (Bray et al., 2001; Warfield et al., 2009).

Mouse-adapted EBOV initially infects macrophages and other mononuclear phagocytes at the site of invasion and in regional lymph nodes. The major target cells of infection are as the same as those in humans, NHPs, and guinea pigs (Davis et al., 1997; Connolly et al., 1999; Zaki and Goldsmith, 1999; Gibb et al., 2001). Viral replication in mononuclear phagocytes in the lymph node, spleen, and thymus and an increase in the number of virus-infected Kupffer cells in the liver were observed by Day 3 after infection. Most mononuclear phagocytes throughout the body appear to be infected and the mice died by Days 5–6.

The adaptation of EBOV to adult mice resulted in 8 amino acid changes in both the coding and non-coding regions of the virus

genome compared to the original wild-typed virus (Ebihara et al., 2006). Nucleotide substitutions leading to amino acid changes were found in VP35, VP24, NP, and L viral proteins. VP24 and VP35 are known as type I interferon (IFN) antagonists and interfere with type I IFN-mediated antiviral response *in vitro* (Bowen et al., 1980; Basler et al., 2000; Bente et al., 2009; Halfmann et al., 2011). VP24 functions as an IFN antagonist by binding karyopherin α and blocking nuclear accumulation of signal transducer and activator of transcription 1 (STAT1; Reid et al., 2007). VP35 is also implicated in blocking type I IFN responses by inhibiting phosphorylation of interferon regulatory factor (IRF) 3 and 7 by the Tank binding kinase-1 and I-Kappa-B kinase epsilon, and sequestering the viral RNA from detection by RIG-I like receptor (Ramanan et al., 2011, 2012). It is considered that there is a significant relationship between filoviral virulence and the ability of the virus to evade the type I IFN-induced antiviral response (van der Groen et al., 1979). The mutations in NP and VP24 genes were found to be critical for acquisition of EBOV virulence in adult mice, but not VP35 mutations (Ebihara et al., 2006). NP is tightly coupled with viral RNA and forms the nucleocapsid complex together with L, VP30, and VP35. Although it is unclear how NP is involved in the IFN response, NP is thought to confer evasion from the IFN-stimulated antiviral responses directly or indirectly in infected mice.

The mutations identified for adaptation of marburgvirus to mice differed from those required for that of ebolavirus. The amino acid mutations were found in VP40, VP35, NP, and VP30 in mouse-adapted RAVV compared to those of the wild-type virus derived from a patient (Warfield et al., 2009). It is still unclear what is the role and necessity of each of the mutations in mouse-adapted RAVV. Further experiments are required to clarify which mutations are critical for adaptation to mice.

Adult mice treated with antibodies against IFN-α/β became susceptible to infections with non-adapted EBOV or SUDV infected via the intraperitoneal route, and to mouse-adapted virus infected via the subcutaneous route (Bray, 2001). Furthermore, non-adapted EBOV, SUDV, MARV, or RAVV caused illness in KO mice lacking type I IFN receptors or the STAT1 protein (Bray, 2001). These results suggest that inhibition of type I IFN response against filovirus infections is critical for pathogenesis in mouse models.

Mice infected with the mouse-adapted filovirus are different from humans and NHPs infected with the original filoviruses in terms of a lack of severe coagulation disorder and fibrin deposition. Mouse models are useful tools for studying basic aspects of replication, pathogenesis, and immune responses and also serve as an irreplaceable platform for evaluating the efficacy of the wide range of the candidate vaccines and therapeutic agents.

GUINEA PIG MODELS

Guinea pigs are susceptible to several arenaviruses, Lassa fever virus, Junin virus, and Guanarito virus and used as animal models for human viral hemorrhagic fevers caused by these viruses (Bowen et al., 1977; Jahrling et al., 1982; Kenyon et al., 1990; Hall et al., 1996). However, infection of guinea pigs with wild-type filovirus usually causes only a transient febrile illness (Simpson et al., 1968; Robin et al., 1971; Bowen et al., 1977). Filoviruses need to be serially passaged in guinea pigs to acquire the ability to cause lethal infection in guinea pigs (Simpson et al., 1968; Robin et al., 1971; Ryabchikova et al., 1996). Guinea pigs inoculated with guinea pig (GP)-adapted virus showed similar symptoms such as fever, anorexia, and dehydration, to those reported in humans and NHPs infected with wild-type filovirus (Simpson et al., 1968; Robin et al., 1971; Connolly et al., 1999). GP-adapted EBOV-infected guinea pigs showed fibrin deposition coincident with decreases in platelet count during the late stage of infection (Connolly et al., 1999). GP-adapted EBOV replicated to high titers in the spleen, liver, adrenal gland, and lung, resulting in viremia in guinea pig models, although the peak titers were less than those demonstrated in NHPs. Viremia in guinea pigs developed within 2 days after inoculation and increased during the course of the disease, reaching a peak on Day 7 ($>10^4$ pfu/ml; Connolly et al., 1999; Subbotina et al., 2010). The guinea pigs infected with the GP-adapted filovirus died on 7–9 days after infection (Simpson et al., 1968; Robin et al., 1971; Connolly et al., 1999; Subbotina et al., 2010).

Histopathological changes in the liver of guinea pigs infected with GP-adapted filoviruses included replication of the viruses in Kupffer cells, multifocal necrosis of hepatocytes, and congestion and destruction of the sinusoid wall, which were also similar to those reported in humans and NHPs infected with wild-type filoviruses (Korb and Slenczka, 1971; Connolly et al., 1999; Ryabchikova et al., 2003). However, infiltrations of inflammatory cells in the liver and other organs were mild or absent (Connolly et al., 1999; Ryabchikova et al., 2003). Lymphoid necrosis was observed in the spleen and lymph nodes of guinea pig models.

Neutrophilia and lymphopenia became detectable in the guinea pig model as early as 2 days after infection and the severity continued to increase over the course of infection (Connolly et al., 1999; Subbotina et al., 2010). However, lymphocyte bystander apoptosis, an important feature in NHPs and mice, was not prominent in guinea pigs (Bray et al., 1999; Connolly et al., 1999; Bradfute et al., 2007). Thrombocytopenia was marked during the late stages of the disease when guinea pigs became moribund and platelets fell from a mean of ~500,000 to <50,000/μl. Fibrin deposition was a late event, beginning only modestly in the liver and spleen on Day 4, with increases in distribution and amount on Days 7–9, coincident with decreases in platelet counts.

Comparative sequence analysis of the complete genomes of the GP-adapted EBOV and wild-type virus showed 8 nucleotide differences, which led to 5 amino acid substitutions; single amino acid mutations in NP and L and 3 mutations in VP24 (Volchkov et al., 2000). Using a reverse genetics approach, it was shown that VP24 had a critical role in the pathogenesis and the amino acid changes in VP24 were essential to achieve EBOV virulence in guinea pigs. VP24 was demonstrated to antagonize IFN signaling by binding host karyopherin α proteins and prevent transport of the tyrosine phosphorylated transcription factor STAT-1 to the nucleus (Reid et al., 2007; Mateo et al., 2010; Zhang et al., 2012). One of the substitutions in VP24 of GP-adapted EBOV

was located in the proximal domain, which was recently shown to be involved in karyopherin binding and required for efficient control of the IFN response (Mateo et al., 2010). However, the mutations associated with EBOV adaptation to the guinea pigs did not affect the ability of VP24 to inhibit IFN signaling (Mateo et al., 2011). VP24 participates in the assembly and/or proper formation of viral nucleocapsids. The lack of virulence of wild-type virus in guinea pigs was associated with an inability of the virus to replicate in and/or be released from hepatocytes and macrophages efficiently (Mateo et al., 2011). Wild-type VP24 is somehow incapable of participating in assembly of viral nucleocapsids in guinea pigs. Mutations in VP24 for adaption to guinea pigs recovered the ability of EBOV to replicate in both macrophages and hepatocytes and to facilitate the systemic spread of the virus.

SYRIAN GOLDEN HAMSTER MODELS

The pathogenesis of rodent-adapted filoviruses differs in some aspects from those of humans and NHPs infected with wild-typed virus (**Table 1**). Fever and cutaneous rash, which are major clinical signs of EHF and MHF in humans and NHPs, are absent in mice infected with mouse-adapted virus. Fever appears in guinea pigs infected with GP-adapted virus, but rash does not develop in these animals. Mice infected with mouse-adapted virus do not consistently display coagulation abnormalities. Compared to mice, guinea pigs infected with GP-adapted virus develop coagulation defects, including a drop in platelet counts and an increase in coagulation time, but coagulopathy (i.e., DIC) are not as marked as that observed in NHPs. Furthermore, lymphocyte apoptosis observed in humans, NHPs, and mice was not determined in the guinea pig model. Because of these differences in the rodent models, some vaccines (e.g., irradiated virion) and therapeutics (e.g., passive immunization with antiserum) that were effective in rodents challenged with adapted virus fail to protect NHPs challenged with wild-type virus (Wahl-Jensen et al., 2012).

Moreover, in the guinea pig model, the lack of available reagents and tools, such as quantitative reverse-transcription polymerase chain reaction (qRT-PCR) and ELISA for cytokine profiling, makes the guinea pig model less desirable. Therefore, the development of other rodent models that better recapitulate EHF and MHF in humans was desired for more relevant pathogenesis studies and high throughput screening of prophylactic and post-exposure treatment prior to their testing in NHPs.

Syrian golden hamster (*Mesocricetus auratus*) is broadly used in animal models for human infectious diseases (Zivcec et al., 2011). Suckling hamsters were susceptible to wild-type MARV but disease was evident in only 40–80% of the animals following either intracerebral or intraperitoneal inoculation (Zlotnik, 1971). The symptoms and the mortality which was up to 90% were observed by inoculation with ninth passage materials in 5–6-week-old hamsters. While the pathological changes in the hamsters are similar to those observed

Table 1 | Comparison of pathological features of different animal models of filovirus infection.

	Mouse	Guinea pig	Hamster	NHP	Human
Virus adaptation	Adapted	Adapted	Adapted	Wild-type	Wild-type
Viremia	High	High	High	High	High[a]
Virulence	High	High	High	High	High[b]
Weight loss	Severe	Severe	No	Severe	Severe[c]
Rash	No	No	No	Yes	Yes[d]
Thrombocytpenia	Yes	Yes	Yes	Yes	Yes[e]
Lymphocyte apoptosis	Yes	Limited	Yes	Yes	Yes[f]
Cytokine response	Yes	Yes	Yes	Yes	Yes[g]
PT	Remained	Increased	Increased	Increased	Increased[h]
PTT/aPTT	Remained	Increased	Increased	Increased	Increased[i]
TT	ND	ND	Increased	Increased	ND
Fibrin deposition in organs	Little	Moderate	Little	Abundant	Observed[j]
Protein C activity	ND	ND	Decreased	Decreased	ND

[a] *Ksiazek et al., 1999; Ndambi et al., 1999; Sanchez et al., 2004; Towner et al., 2004; Kuhn, 2008.*

[b] *Isaacson et al., 1978; Piot et al., 1978; Smith et al., 1978; Bwaka et al., 1999; Sanchez et al., 2007; Kuhn, 2008.*

[c] *Bwaka et al., 1999; Kuhn, 2008.*

[d] *Isaacson et al., 1978; Smith et al., 1978; Bwaka et al., 1999; Sanchez et al., 2007; Kuhn, 2008.*

[e] *Sanchez et al., 2007; Kuhn, 2008.*

[f] *Baize et al., 1999.*

[g] *Baize et al., 1999, 2002; Sanchez et al., 2007.*

[h] *Sanchez et al., 2007; Kuhn, 2008.*

[i] *Sanchez et al., 2007.*

[j] *Dietrich et al., 1978.*

Abbreviation; PT, prothrombin time; PTT, partial thromboplastin time; APTT, activated partial thromboplastin time; TT, thrombin time ; ND, no data.

in other animal models including patients, encephalitis, which is not observed in other animals, were constantly demonstrated in all suckling hamsters, irrespective of route of inoculation, and in adult hamsters, when the virus was inoculated intracerebrally.

The Syrian golden hamster model was developed for EHF based on infection with mouse-adapted EBOV. Six-week-old hamsters infected intraperitoneally with 10^3 focus forming unit (ffu) of mouse-adapted EBOV started to show clinical signs of disease, including ruffled fur and decreased activity, by Day 3 after infection and succumbed to disease within 4–5 days after infection. When inoculated subcutaneously, mouse-adapted virus failed to produce lethal infection in hamsters in the same way as the mouse model. Mouse-adapted EBOV-infected hamsters showed severe coagulopathy with prolonged PT, aPTT, and thrombin time (TT), in the late stage of infection (Ebihara et al., 2013). Other factors, including increased fibrinogen, decreased protein C activity, thrombocytopenia, and coagulation disorder were observed in the hamster model. The target organs were the mesenteric lymph node, spleen, liver, and adrenal gland. In the mesenteric lymph node, the target cells were the macrophages and dendritic cells (DCs). The viral antigens were found in macrophages, marginal reticular-like cells, and DC-like cells in the spleen, and Kupffer cells and hepatocytes in the liver. Histopathological changes, including inflammatory cell infiltration, cellular necrosis, and apoptosis, were mainly noted in the lymphoid organs (spleen and mesenteric lymph node) and liver. These pathological changes were similar to those demonstrated in NHPs and other rodent models (Baskerville et al., 1978; Fisher-Hoch et al., 1992; Jahrling et al., 1996; Ryabchikova et al., 1996, 1999; Bray et al., 1999; Connolly et al., 1999; Warfield et al., 2009). Fibrin deposits in liver sinuses, which are a hallmark of EBOV infection in humans and NHPs, were detected to a lesser extent in the hamster model (Ebihara et al., 2013). Suppression of type I IFN that enhances viral replication in target cells and contributes to lethal disease was observed (Ebihara et al., 2013).

It has been demonstrated that the mouse-adapted EBOV-based Syrian golden hamster model shows the most similar clinical and pathological features, including coagulation abnormalities, to those observed in humans and NHPs infected with wild-type EBOV.

NON-HUMAN PRIMATE MODELS

Although guinea pigs, mice, and hamsters models have been developed to study EHF and MHF as stated above, the rodent models are not ideal because mice and guinea pigs, except a novel hamster model, do not entirely exhibit coagulation disorders that are associated with human and NHPs filovirus infections (Table 1). Additionally the bystander death of large numbers of uninfected lymphocytes due to apoptosis that are hallmark features in filovirus-infected humans and NHPs is not present in infected guinea pigs. In mouse models, the bystander lymphocyte apoptosis was reported, but the process and morphology of lymphocyte apoptosis was different from those of filovirus-infecting humans and NHPs (Bradfute et al., 2007).

In NHP models, apoptosis was the primary reason for lymphocyte death, but the lymphocyte death in mouse models appeared to occur by apoptosis and apoptosis-like programmed cell death. Furthermore, NHPs are lethally infected with non-adapted filovirus isolates resulting in pathophysiology similar to that demonstrated in humans, although rodent models required serial passages of the virus for adaptation to produce lethal disease. Because of the aforementioned disadvantages and differences in the disease pathology, NHPs remain the most useful and reasonable model of EHF and MHF despite practical and ethical considerations leading to the restriction of experiments.

MARBURGVIRUS INFECTION IN NHPs

The first documented outbreak of MHF was associated with wild-caught African green monkeys (*Chlorocebus aethiops*) in Uganda and imported to Marburg and Frankfurt, Germany, and to Belgrade, Serbia Montenegro, former Yugoslavia, in 1967 (Martini, 1971). Since the first outbreak of MHF originated from the wild-caught African green monkeys, this species was an obvious choice for an animal model of MHF. At that time, rhesus macaques (*Macaca mulatta*) were found to be equally susceptible to infection and showed symptoms after inoculation with MARV (Hass and Maass, 1971). Cynomolgus macaques (*Macaca fascicularis*) were also well characterized as an MHF model (Hensley et al., 2011). After an incubation period of 2–6 days, the monkeys showed febrile illness, anorexia, diarrhea, skin rash, and hemorrhagic manifestations by any routes of MARV-inoculation (Simpson et al., 1968; Simpson, 1969; Murphy et al., 1971; Geisbert et al., 2007; Alves et al., 2010; Hensley et al., 2011). Death occurred by 6–13 days post-infection after a sudden decrease in body temperature and the mortality rate was almost 100%. It was shown that reducing the virus inoculum led to delayed onset of the disease and longer time to death without reduction in mortality rate (Hass and Maass, 1971). In the macaques, petechial rashes on the forehead, chest, axillae, and groins were prominent and resembled the rashes that appeared in patients with MHF, but intriguingly the rashes were not seen in African green monkeys (Simpson, 1969).

A marked lymphocytosis was observed at the beginning of the illness (Simpson et al., 1968; Simpson, 1969; Gonchar et al., 1991; Spiridonov et al., 1992; Johnson et al., 1996; Geisbert et al., 2007). Thrombocytopenia and leukocytosis due to increased neutrophilia were prominent on 5–6 days after infection (Hensley et al., 2011). Changes in coagulation systems, such as a decrease in circulating levels of protein C, an increase in levels of circulating D-dimer and fibrin deposition in tissues were noted at late stages of the disease (Geisbert et al., 2007; Hensley et al., 2011). The pathological changes in liver including multifocal necrosis of the parenchyma cells, and lymphocyte apoptosis in lymphoid tissues were prominent (Geisbert et al., 2000). Monocyte/macrophages and DCs in the lymphoid tissues as well as Kupffer cells and sinusoids lining cells in the liver were the primary target cells for infections with MARV (Hensley et al., 2011). The infection then progressed to parenchymal cells in the liver, adrenal gland, and high endothelial venules in lymphoid tissues. Finally, the infection spread to endothelial cells in a variety